Wetting Behavior of Cerium Oxide Films Grown by Pulsed Laser Deposition

Daniel Li

Department of Materials Science and Engineering, University of Illinois at Urbana-Champaign, Champaign, IL

Jeremiah T. Abiade

Department of Mechanical Engineering, University of Illinois at Chicago, Chicago, IL

Abstract

Metallic oxides with particular wettability characteristics have far reaching applications in corrosion prevention, liquid conveyance, and self-cleaning surfaces, among other fields. Cerium (Ce) oxide films were deposited onto a silicon substrate by pulsed laser deposition from a cerium target in the presence of O_2 gas at room temperature, 300 degrees Celsius, and 700 degrees Celsius. The oxygen pressure was varied amongst the samples to change the relative concentration of Ce^{3+} and Ce^{4+} films. The samples were then characterized by x-ray photoelectron spectroscopy (XPS) to determine the valency of Ce and the stoichiometry of the films. Water contact angle measurements over time were completed with use of a goniometer. The contact angle varies initially but for most samples saturate at roughly 90 degrees, aside from those grown at an oxygen partial pressure of .3mTorr or greater. Samples grown at higher deposition temperature had more uniform wetting characteristics than those grown at lower temperatures. This information may assist the continued study of the intrinsic hydrophobic properties in rare earth oxides and their potential applications in industry.

Keywords: Pulsed laser deposition, cerium oxide, hydrophobicity

I. Introduction

Surface engineering often involves directing the wettability of a material, divided into two desirable categories depending on the situation desired: hydrophobicity and hydrophilicity[1]. Hydrophobicity is of particularly great interest as the ability to repel water could have a wide range of applications in power and industrial plants; water condensation is a very common aspect of cooling processes for electric and water facilities. A hydrophobic surface would prevent the formation of a boundary layer within the water conduit and eliminate the boiling of nucleation sites, allowing for much higher heat transfer efficiency[2]. Another possible attraction is the ability of hydrophobic surfaces to reduce ice and snow accumulation in cool environments, allowing the water to roll off before the water crystallizes[3]. Large scale, industrial application is still unfeasible despite past and ongoing research on properties of substrates that will make water behave in a purposeful manner[4]. Commercial options are limited by the hydrophobic materials' mechanical and thermodynamic fragility[5], though short term devices such as disposable microfluidics, degradable sutures, and temporary surface enhancements are viable since deterioration is not a major obstacle. Parkin et al.[6] was able to prepare superhydrophobic elastomeric surfaces through aerosol-based deposition that produced high contact angle and low hysteresis, while Cao et al.[7] utilized electro-deposition to create microstructured surfaces that mimicked the lotus leaf. Other polymer-based coatings currently used in anti-fogging glass and self cleaning ceramics are relatively soft with low adhesion and durability[5, 8]. Though these examples have proven effective under standard atmospheric conditions, they degrade under high stress -pressure, heat, and abrasion. Furthermore, fabrication of these traditional hydrophobic films requires caustic chemicals mixtures that create environmental and health concerns.

Hydrophobic, liquid-films such as SLIPS or liquid-glide offer a unique yet simple solution by eliminating contact line pinning and contact angle hysteresis, but they are easily exposed to contamination from dust and impurities from atmosphere exposure, thus decreasing the coating's effectiveness[8].

Hydrophobicity and hydrophilicity together fall under the umbrella description of wettability [9]. The presence of either phenomenon may be explained by wetting behavior, which may be classified by measuring water contact angle (WCA) on the surface of interest[10]. Water molecules on an interface may choose to interact with one another and ball up through cohesion, or they may spread out and interact with the surface due to water's adhesive properties[11]. The first extreme is complete non-wetting, where liquid water ideally makes no contact with the substrate. In contrast, complete wetting occurs when a liquid spontaneously forms a low angle sheen film over a surface. A contact angle of 0 degrees is considered perfect wetting, whereas 180 degrees is perfect non-wetting; a WCA between 0 and 90 degrees is considered to have high wettability (hydrophilic); whereas a WCA between 90 and 180 degrees has low wettability (hydrophobic) [12]. The first investigations governing these properties for ideal (perfectly flat and homogenous) solids were explored in the early 1800s. Young and Laplace found that interacting materials may be described by surface tension based on the internal cohesive forces where the influence of roughness, swelling, and molecular heterogeneity may be ignored. Ideal surface specific energy may be described as a force per unit length between two phases: solid/gas (SG), solid/liquid (SL), or liquid/gas (LG). These forces apply along an interface in such a manner that the overall surface energy is minimized. Young's equation below relates these surface energies with theta being the contact angle between the solid and the water[13]. This allows one to predict

the WCA from knowledge of the surface energies, and vice-versa.

$$\gamma SG = \gamma SL + \gamma LG cos\theta$$

Surface free energy and polarity combined are directly responsible for its molecular orientation[14]. Metallic and ceramic surfaces are generally hydrophilic as they have many unsaturated polar sites. These sites will try to form full octets by forming hydrogen bonds at the interfacial plane. K. Varanasi et al.[15]demonstrated that the lanthanides transition metal oxides, or rare earth metal oxides (REOs), have intrinsic hydrophobic properties due to their uniquely organized electronic structure[16]. The inner, unfilled 4f orbital is shielded from the environment by an outer, full $5s^2p^6$ shell. This decreases the tendency for water molecules to form hydrogen bonds at the interface, and instead form pillar-like supports protruding perpendicularly from the surface. Therefore only one hydroxyl group points to the substrate, while the other three vectors form internal hydrogen bonds[17].

REOs, unlike popular commercial hydrophobic polymeric additives, have the ability to retain their hydrophobic properties even after harsh treatments and damage[18]. Therefore, these REOs may be applied as a coating or used in bulk form. Here we take a particular interest to cerium oxide since it has many favorable characteristics: chemical stability, high adhesion, thermal transfer, wide band gap, wear resistance, large refractive index, and relatively low cost[19]. Current ceria thin film applications include metallic corrosion prevention coatings, redox reaction catalysis, and use in compatible semiconductor layers[20]. It may act as a buffer between silicon and superconducting materials exposed to high temperature and pressure. Ceria films are also used in UV filters for optical-sensitive devices due to its transparency in the visible and infrared light spectrum[21]. There are a variety of methods to fabricate ceria thin films, including

thermal evaporation, chemical vapor deposition, and ion-beam assisted deposition[22]. Among those procedures, pulsed laser deposition (PLD) is a reliable technique as it preserves the stoichiometry of the target, and allows for variation in composition by adjusting laser fluence, energy density, basal pressure, ambient gas pressure, temperature, and frequency[23]. There are studies that indicate cerium oxides (ceria) to have a high WCA, but the actual mechanism for this behavior has yet to be determined[24]. Cerium displays three oxidation states, +2, +3, and +4, but it is mainly the +3 and +4 states that appear, forming cerium (III) oxide (Ce_2O_3) and cerium (IV) oxide (CeO_2). In the presence of oxygen, Ce_2O_3 can be converted to the +4 oxidation state through the following equation:

$$2\,Ce_2O_3 + O_2 \rightarrow 4\,CeO_2$$

Conversely, CeO2 may be reduced to Ce2O3 with carbon monoxide:

$$2\,Ce_2O_3 + CO \rightarrow Ce_2O_3 + CO_2$$

Not unexpectedly, the ratio between the +3 and +4 oxidation state is tunable based on oxygen partial pressure at the time of deposition. The cubic fluorite structure of CeO_2 is more stable at standard temperature and pressure than the hexagonal structure of Ce_2O_3, and is known to have strong resistance to mechanical and chemical attack. Utilizing these properties may present a viable option to form a robust hydrophobic coating compatible with electronics, antifogging optics, and other pre-established devices. This information will aid in finding a chemically stable, non-hazardous oxide that can be reliably deposited on to a substrate. This will ultimately lead to cost-effective assembly of nanostructured, superhydrophobic products using non-toxic materials.

In this letter, we report on the wettability of ceria thin films through goniometer water contact angle measurements to examine the extent of hydrophobicity at each oxygen partial pressure. Composition was analyzed through x-ray photoelectron spectroscopy (XPS) to confirm the atomic ratio of cerium to oxygen at the particular oxidation states to find the relative amount of Ce_2O_3 compared to CeO_2.

II. Experimental Procedures

A rotating rod cerium target (99.9% purity, 1 in. diameter, 0.5 in. thickness) produced by Super Conductor Materials was deposited onto approximately 0.5 mm x 0.5 mm x 0.05 mm polished (100 oriented N-type doping) silicon substrates manufactured by CrysTec. The target had been synthesized by low-stress powder compression prior to acquisition. Pulsed laser deposition was accomplished using a 248 nm KrF excimer laser, which operates approximately 6 feet away from the deposition chamber. It was programmed to pulse 5000 times at 4.5 J/cm^2 energy at a frequency of 5 Hz with a 15 ns pulse duration for every deposition.

Prior to deposition, the cerium target was sanded and cleaned to ensure coherent ablation. Silicon substrates were cleaned for five minutes by sonification in solutions of acetone, methanol, and isopropanol. The substrates were subsequently dried using nitrogen gas and attached to the deposition stage by either a metal clip or silver paste. These processes were done at room temperature. Afterwards, the substrate holder was heated to 300 degrees Celsius over 30 minutes where it remained at that temperature until the deposition finished. The same process was completed at 700 degrees Celsius, and samples completed at room temperature were left unheated. Target pre-ablation was done at a basal pressure of ~5e-6 torr with 1000 pulses at 5Hz.

The target was rotated in the axial and lateral direction to prevent uneven pitting. Oxygen gas was introduced shortly after pre-ablation and its pressure remained at constant levels throughout the deposition. There was a 6.2 cm gap between the target and the substrate. The substrate was then allowed to cool to room temperature over 30 minutes to prevent cracking and delamination. After the deposition completed, the O_2 was vented and the sample stored for later characterization. A complete index of the samples can be found on Table 1. XPS analysis was completed by technicians from the Laboratory for Oxide Research and Education (LORE).

Table 1. Description of the PLD thin films created

Room Temperature	**300 Degrees Celsius**	**700 Degrees Celsius**
2.5 E-2 Torr (T)	**No Oxygen**	**2.2 E-2 T**
7.5 E-2 T	**2.1 E-1 T**	**7.4 E-2 T**
2.5 E-3 T	**6.2 E-2 T**	**2.1 E-2 T**
7.5 E-3 T	**4.7 E-3 T**	**7.5 E-3 T**
	8.1 E-4 T	**7.2 E-4 T**

XPS (KRATOS Manufacturing) was completed and preliminary peak deconvolution was done on XPSPEAK 4.1. As with elements with d subshells, CeO_2 has three peaks made of the characteristic 3d5/2 and 3d3/2 spin orbital splitting. Overall peak fitting involve the separation of heavily overlapped oxidation states.

A goniometer was used for the wettability measurements. 4 microliters were dropped onto the sample with a 10 microliter syringe. The droplet was projected onto an external display and the contact angle measured with the on-screen protractor. A WCA measurement was taken from each side of the 2D image and averaged to ensure the results were consistent and to account

for possible hysteresis. Water contact angle was measured at varying time intervals after the substrate was allowed to cool to room temperature.

III. Results and Discussion

For all of the samples listed in figures 1, 2, and 3, the WCA increased over time, though some deviated more than others. Samples created at lower oxygen pressure eventually stabilized to 90 degrees. Water contact angles varied initially between 20 to 60 degrees but generally level to 85-90 degrees after a week. This suggests that ceria undergoes additional oxidation in atmospheric oxygen once deposition has finished. However, samples made at room temperature (Fig. 1) and 300 degrees (Fig. 2) oxygen partial pressures higher than 3 E-2 Torr, aside from the sample made in vacuum only, did not increase to over 60 degrees. However, all 700 degrees thin films (Fig. 3) did reach 90 degrees regardless of deposition temperature over 14 days. Further investigation needs to be done on the effect of temperature on surface morphology of ceria thin films, and its role in affecting hydrophobicity. XPS confirms that the surface oxidation does differ by partial oxygen partial pressure, as expected, and is largely unaffected by deposition temperature. Figure 4 displays the XPS of Ce 3d grown at an oxygen partial pressure of 7.5 E-3 T, while Figure 5 displays the XPS of Ce 3d grown at an oxygen partial pressure of 2.1 E-3 T. These XPS peak fits of two select samples were deposited at the same temperature and suggest drastically different oxidation states. This data supports the idea that samples created at higher oxygen partial pressure have a greater amount of Ce (4+) oxidation state, while those created at a lower oxygen partial pressure have a greater amount of the Ce (3+) oxidation state. Both had roughly the same WCA, approximately 90 degrees, after they stabilized over a week of time. Despite indications of different oxidation states, it does not seem to play a significant in how hydrophobic the ceria thin film is. Future work needs to be done in creating a pure cerium and

cerium dioxide XPS standard to use as a basis of comparison for binding energy and peak intensity. This will allow full deconvolution of cerium 3d peaks to determine stoichiometry and the relative amounts of each oxidation state. Depositions at oxygen partial pressures below 3 E-2 T is preferable for hydrophobicity, and even lower oxygen partial pressures should be used if short term sensitivity is a concern, as samples grown at higher oxygen partial pressures had lower initial water contact angles. WCA differences measured from one side compared to another of a water droplet on the same sample may be explained by height fluctuations and non-uniformity, but are generally negligible. Both these sources of concern may be due to imperfections when operating at the nano-length scale. Despite the best controls, our silicon substrates will not be coated with a completely flat layer, especially since PLD is very directional in nature and sensitive to plume size. At the contact line, there are sharp edges and turns which allow for hysteresis, a range of plausible angles, may be observed. Another cause of concern is the lack of uniformity and homogeny. There is likely non-uniform nucleation that allowed different patches on the sample having different hydrophobicities, and therefore hysteresis, but this should be negligible. Film growth was relatively stable, though some areas displayed scattering and inhomogeneous nucleation. Some areas were slightly thicker than in other areas, but the substrate size was relatively small to defer this problem.

Figure 1. WCA over time of samples created at room temperature

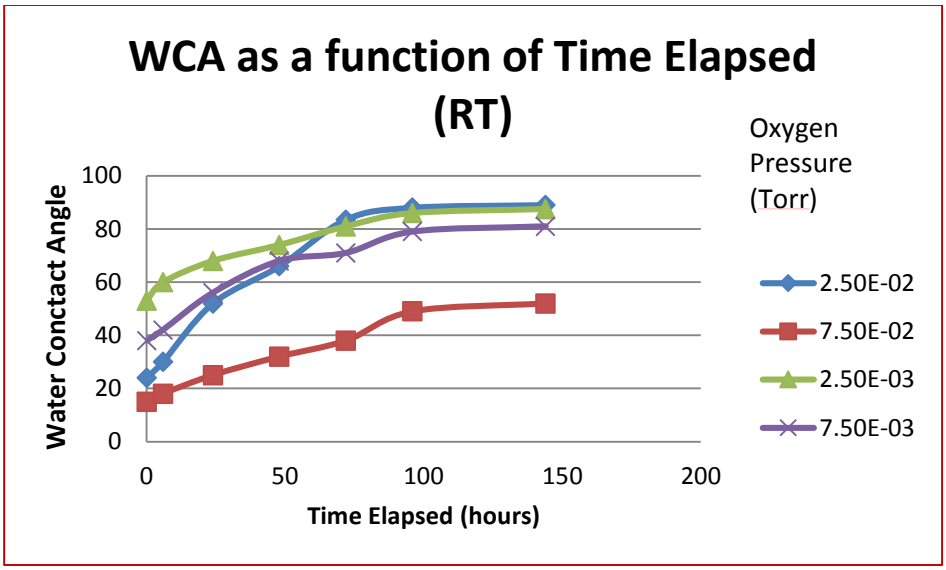

Figure 2. WCA over time for samples created at 300 degrees Celsius

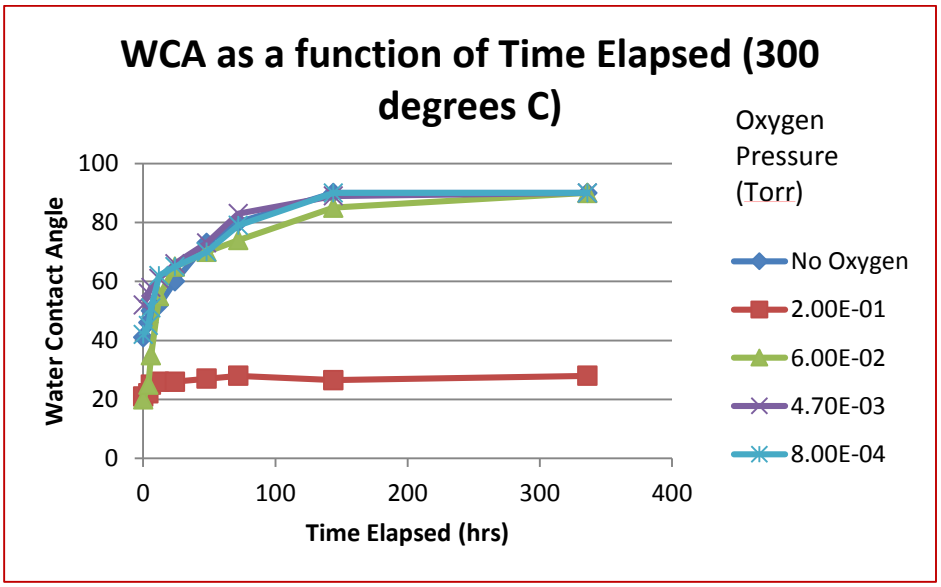

Figure 3. WCA over time of samples created at 700 degrees Celsius

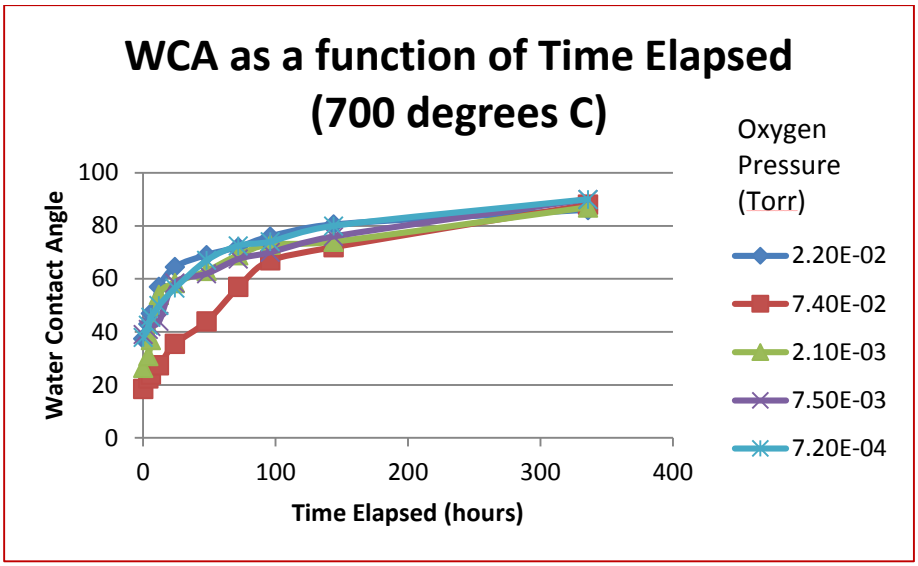

Figure 4. XPS of Cerium 3d for the 7.5 E-3 T, 700 degree Celsius sample

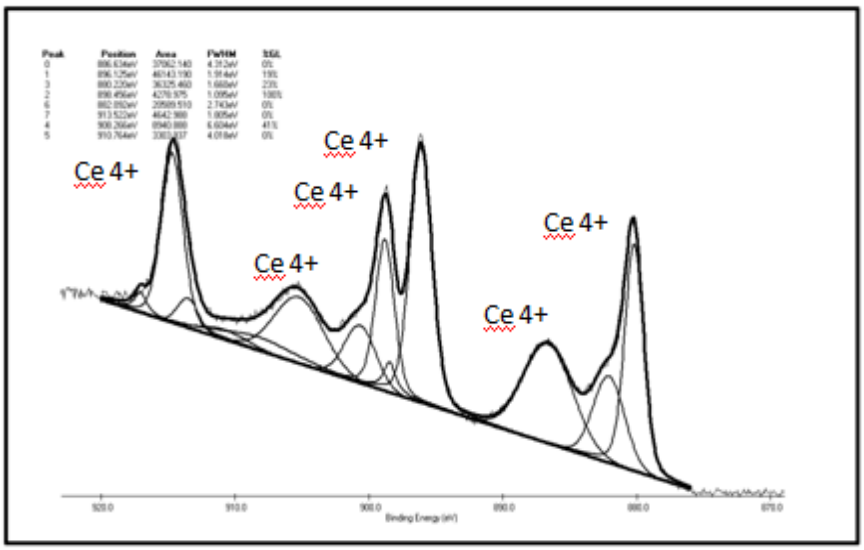

Figure 5. XPS of Cerium 3d for the 2.1 E-3 T, 700 degrees Celsius sample

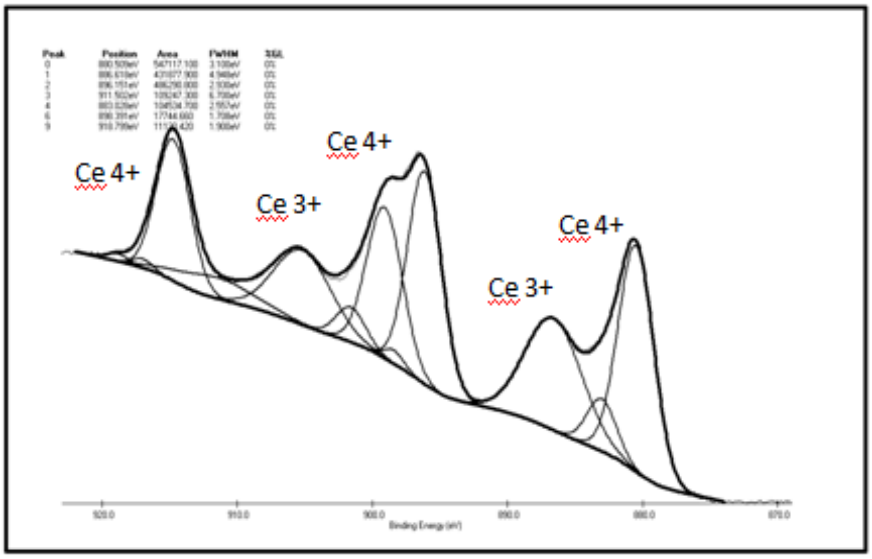

IV. Conclusion

Ceria thin films were prepared by PLD under varying oxygen partial pressures and deposition. Water contact angle measurements were taken over the course of a week and select samples were characterized by XPS to determine stoichiometry. Hydrophobicity was found to be optimized by controlling the Cerium's oxidation state by changing the deposition temperature and oxygen partial pressure, but ultimately samples that were created below 3 E-2 oxygen partial pressure all increased to roughly 90 degrees over the course of a week. XPS data suggests that oxygen partial pressure does indeed influence the cerium oxidation states, but this may not be highly influential in determining hydrophobicity of the thin film.

V. Acknowledgements

This opportunity would not be made possible without the financial support of the National Science Foundation. EEC-NSF Grant #1062943 is gratefully acknowledged. I thank Professors G. Jursich and C.G. Takoudis for organizing the REU Program, as well as the rest of the REU staff. I appreciate my advisor Professor Jeremiah Abiade for his guidance, as well as graduate students Riad Alzeghier and Jelani Hannah for assistance in the lab. Finally, I want to acknowledge the Takoudis group for use of their goniometer.

References

[1] Joanne Deval *et al* "Reconfigurable hydrophobic/hydrophilic surfaces in microelectromechanical systems (MEMS)" 2004 *J. Micromech. Microeng.* 14 91

[2] Anand, Sushant, Adam Paxon, and Kripa K. Varanasi. "Enhanced Condensation on Lubricant-Impregnated Nanotextured Surfaces." *American Chemical Society* 6.11 (2012): 10122-0129. *ACS Nano*. Apr.-May 2012.

[3] Cao, Liangliang, Andrew K. Jones, and Vinod K. Sikka. "Anti-Icing Superhydrophobic Coatings." *Langmuir Letter* (2009): n. pag. American Chemical Society, Sept. 2009.

[4] Nakajima, Akira. "Design of Hydrophobic Surfaces for Liquid Droplet Control." *Asia Materials* 3.55 (2011): 49-56. *Nature*. NPG, 19 May 2011.

[5] Liu, Kesong, and Lei Jiang. "Metallic Surfaces with Special Wettability." *Nanoscale* 3.3 (2011): 825-38. RSC Publishing, 11 Jan. 2011.

[6] Crick, Colin R., and Ivan P. Parkin. "A Single Step Route to Superhydrophobic Surfaces through Aerosol Assisted Deposition of Rough Polymer Surfaces: Duplicating the Lotus Effect." *Journal of Materials Chemistry* 19.8 (2009): 1074-079

[7] Cao, Feng, Zisheng Guan, and Dongxu Li. "Preparation of Material Surface Structure Similar to Hydrophobic Structure of Lotus Leaf." *Journal of Wuhan University of Technology-Mater. Sci. Ed.* 23.4 (2008): 513-17. Aug. 2008

[8] Wong, Tak-Sing, Sung Hoon Kang, and Sindy K.Y. Tang. "Bioinspired Self-repairing Slippery Surfaces with Pressure-stable Omniphobicity." *Nature.com*. Nature Publishing Group, 21 Sept. 2011. Web. 08 July 2013.

[9] Quéré, David. "Wetting and Roughness." *Annual Review of Materials Research* 38.1 (2008): 71-99. *Review in Advance*. Annual Review of Materials Research, 7 Apr. 2007.

[10] Fowkes, F. Contact Angle, Wettability and Adhesion, American Chemical Society, 1964

[11] McCarthy, T. A Perfectly Hydrophobic Surface, J. Am. Chem.Soc., 2006, 128, 9052.

[12] Tanford, C. "The Hydrophobic Effect, Wiley. 1973

[13] Young, Thomas. "An Essay on the Cohesion of Fluids." *Philosophical Transactions of the Royal Society of London (1776-1886)* 95.1 (1805): 65-87. Royal Society Publishing.

[14] Giovambattista, N., Debenedetti, P. G. & Rossky, "Enhanced surface hydrophobicity by coupling of surface polarity and topography. Proceedings of the National Acaddemy of Sciences. USA 2009, 106 no.36,

[15] Azimi, Gisele, Rajeev Dhiman, Kwon Hyuk-Min, Adam T. Paxton, and Kripa K. Varanasi. "Hydrophobicity of Rare-earth Oxide Ceramics." *Nature Materials* 12.4 (2013): 315-20. Nature Publishing Group, 20 Jan. 2013.

[16] Adachi, G., Imanaka, N. & Kang, Z. C. Binary Rare Earth OxidesCh. 2 (KluwerAcademic, 2004).

[17] K.Tsukuma, M. Shimada, "Strength, Fracture Toughness and Vickers Hardness of CeO2 Stabilized Tetragonal ZrO2 Polycrystals," *Journal of Materials Science*, 20 (1985), 1178-1184.

[18] Beie, H.-J., and A. Gnörich. "Oxygen Gas Sensors Based on CeO2 Thick and Thin Films." *Sensors and Actuators B: Chemical* 4.3-4 (1991): 393-99.

[19] M. F. Stroosnijder, V. Guttmann, T. Fransen, J. H. W. de Wit, "Corrosion of Alloy 800H and the Effect of Surface Applied CeO2 in a Sulfidizing Oxidizing Carburizing Environment at 700 degree-C", *Oxidation of Metals*, Vol. 33, Nos. 5/6, 1990

[20] Patsalas, P., S. Logothetidis, and C. Metaxa. "Optical Performance of Nanocrystalline Transparent Ceria Films." *Applied Physics Letters* 81.3 (2002): 466.

[21] A.E. Hughes, J.D. Gorman, P.J.K. Patterson, R. Carter, Surface Interfacial Analysis 1996, 24, 634-640

[22] Mohandas, E., G. Balakrishnan, and S. Tripura Sundari. "A Study of Microstructural and Optical Properties of Nanocrystalline Ceria Thin films Prepared by Pulsed Laser Deposition." *Elsevier*(2010): 2520-526. *Science Direct*. Thin Solid Films, 10 Dec. 2010.

[23] Jiang, Keren. "Fabrication and Catalytic Property of Cerium Oxide Nanomaterials."*Chemistry Thesis* (2011): 1-73. University of Nebraska- Lincoln, Jan. 2011.

[25] Martínez, L., E. Román, J.l. De Segovia, S. Poupard, J. Creus, and F. Pedraza. "Surface Study of Cerium Oxide Based Coatings Obtained by Cathodic Electrodeposition on Zinc." *Applied Surface Science* 257 (2011): 6202-207.